Reversible Cross-Linking, Microdomain Structure, and Heterogeneous Dynamics in Thermally Reversible Cross-Linked Polyurethane as Revealed by Solid-State NMR

ARTICLE *in* THE JOURNAL OF PHYSICAL CHEMISTRY B · JANUARY 2014

Impact Factor: 3.3 · DOI: 10.1021/jp409893f · Source: PubMed

8 AUTHORS, INCLUDING:

Rongchun Zhang
University of Michigan
27 PUBLICATIONS **123** CITATIONS
SEE PROFILE

Chen Shengli
Nankai University
2 PUBLICATIONS **3** CITATIONS
SEE PROFILE

Pingchuan Sun
Nankai University
119 PUBLICATIONS **1,543** CITATIONS
SEE PROFILE

THE JOURNAL OF PHYSICAL CHEMISTRY B

Article

pubs.acs.org/JPCB

Reversible Cross-Linking, Microdomain Structure, and Heterogeneous Dynamics in Thermally Reversible Cross-Linked Polyurethane as Revealed by Solid-State NMR

Rongchun Zhang,[‡] Shen Yu,[†] Shengli Chen,[†] Qiang Wu,[†] Tiehong Chen,[†] Pingchuan Sun,*[,†] Baohui Li,*[,‡] and Datong Ding[‡]

[†]Key Laboratory of Functional Polymer Materials, Ministry of Education, College of Chemistry, Nankai University, and Collaborative Innovation Center of Chemical Science and Engineering (Tianjin), Tianjin, 300071, P. R. China

[‡]School of Physics, Nankai University, Tianjin, 300071, P. R. China

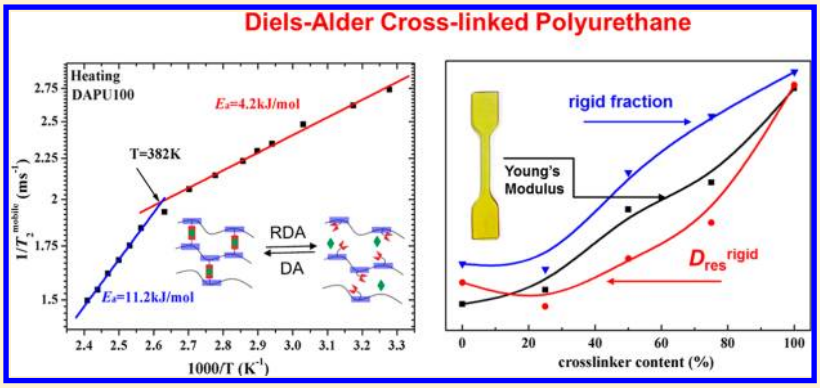

ABSTRACT: Polyurethane material is widely utilized in industry and daily life due to its versatile chemistry and relatively easy handling. Here, we focused on a novel thermally reversible cross-linked polyurethane with comprehensive remarkable mechanical properties as reported in our recent work (*Adv. Mater.* **2013**, *25*, 4912). The microphase-separated structure and heterogeneous segmental dynamics were well revealed by T_2 relaxometry experiments, which was also first utilized to in situ monitor the reversible cross-linking associated with Diels–Alder (DA) and retro-Diels–Alder (RDA) reactions. On the basis of T_2 relaxometry results, we determined the actual temperature of the (R)DA reaction as well as the corresponding activation energies of the motion of soft segments. Besides, the roles of the temperature and cross-linker contents on the microdomain structure and dynamics are discussed in detail. It is found that the microphase separation is enhanced by the increase of temperature as well as the incorporation of cross-linkers. Also, the polyurethane samples are still thermal-stable even at a high temperature beyond the disassociation of the cross-linkages. Furthermore, Baum–Pines and three-pulse multiple-quantum NMR experiments are utilized to investigate the heterogeneous structures and dynamics of the mobile and rigid segments, respectively. Both the results obtained from the T_2 relaxometry and multiple-quantum NMR experiments are in good agreement with the macroscopic mechanical properties of the polyurethane. Finally, it is also well demonstrated that proton T_2 relaxometry combined with multiple-quantum NMR is a powerful method to study the heterogeneous structures and dynamics of a multiphase polymer system.

INTRODUCTION

Over the past few decades, there has been great interest in the dynamic characteristics where certain types of dynamic bonds or interactions could be disassociated and reassociated under specific conditions.[1−4] Such environment-responsive ability renders the rapid development of structurally dynamic polymers that could adapt special microstructures as a response to the external stimulus.[5] In particular, the reversible Diels–Alder (DA) reactions[6−8] under mild conditions have received wide attention, as the DA cycloadducts often provide the materials with thermally self-healing or self-repairing properties.[9−11] The DA reactions of polymers incorporating furan (diene) and maleimide (dienophile) groups are widely studied,[12−16] where the furan/maleimide DA adduct exhibits a lower temperature of decoupling through its retro-DA (RDA) reactions, and thus to pave the way to the applications such as self-healing or recyclable materials. For the slow polymerization reactions, where the reversible furan/maleimide groups were in the reactive monomers, the DA kinetics could be monitored and characterized by solution NMR, UV, or IR spectroscopy.[17−19] However, for the furan/maleimide groups attached on the linear polymer backbones, the DA reactions are so fast,

Received: October 5, 2013
Revised: January 7, 2014
Published: January 8, 2014

   dx.doi.org/10.1021/jp409893f | *J. Phys. Chem. B* 2014, 118, 1126−1137

rendering its characterization difficult.[10,20] Therefore, it still remains a challenge to in situ monitor the (R)DA reactions at present, which will be addressed in this paper.

Recently, inspired by nature, we synthesized a thermally reversible cross-linked polyurethane utilizing reversible DA reactions, which has a comprehensively remarkable enhancement of mechanical properties, excellent recyclability, and remending ability, as reported in our recent work.[21] For many decades, segmented polyurethane materials have enjoyed great popularity in wide-ranging applications due to their tunable properties and ease for processing. The intrinsic hierarchical microstructures of polyurethane resulted from the phase separation between the hard segments, with high glass transition (T_g) or melting temperature (T_m), and the flexible soft components, with a low T_g, make it have the advantages of both rubbers and plastics.[22−24] At room temperature, the soft domains are in a rubbery state while the hard domains are glassy or semicrystalline; therefore, in general, the extensibility of the segmented polyurethane increases with the soft segment content, whereas the stiffness and strength increase with the hard segment content.[25−30] In most cases, the thermoplastic polyurethanes are processable but with poor resistance ability to solvents. On the other hand, covalent cross-linked thermosetting polyurethanes are not easy to process, reshape, or repair when damaged once synthesized, even though they provide superior mechanical properties and solvent resistance. Thus, recyclable and remendable polymers based on thermally reversible Diels−Alder (DA) reactions for cross-linking polymers has attracted considerable recent attention due to their great potential in processing, reshaping, thermally self-repairing, as well as extending the service life of materials.[15,16,31] Our recent work[21] successfully incorporated the reversible cross-linked dynamics bonds utilizing DA reaction into the microphase-separated polyurethane system to enhance its mechanical properties, resistance to solvents, as well as processability.[32] Therefore, it is quite significant to well establish the relationship between the heterogeneous microdomain structures as well as corresponding segmental dynamics and the excellent mechanical properties, and thus to provide insight into the design of new high performance polymer materials.

In this paper, we have systematically investigated the reversible DA cross-linking as well as the microphase-separated structures and segmental dynamics related to the macroscopic mechanical properties in our polyurethanes. The inverse decay time constant of mobile FID signal $1/T_2^{mobile}$ (T_2^{mobile} is the apparent transverse relaxation time of the mobile segments), obtained from the T_2 relaxometry analysis, is for the first time utilized to in situ monitor the (R)DA reactions, where the actual temperatures of (R)DA reactions are determined as well as the activation energy for the motions of soft segments. Besides, T_2 relaxometry also enables us to determine the fraction of rigid, interphase, and mobile components as well as their corresponding apparent spin−spin relaxation time T_2 reflecting the individual mobility in such a phase-separated system. The microphase separation is enhanced by the incorporation of cross-linker as well as the increase of temperature, as revealed by the SAXS and NMR experiments. Our prepared polyurethane is also proved to be thermal-stable even at a high temperature beyond the disassociation of DA cross-linkages. Multiple-quantum (MQ) NMR further revealed the heterogeneous structure and dynamics in soft and hard domains, and could also be used to prove the disassociation of cross-linkages at high temperatures. Both the T_2 relaxometry and MQ NMR results correspond well to macroscopic mechanical properties of the polyurethane. Therefore, our studies provide a way of understanding the macroscopic mechanical properties of reversible cross-linked polyurethanes at a molecular level. And it is well demonstrated that T_2 relaxometry combined with MQ NMR is a powerful method for investigating the heterogeneous structures and dynamics of a multicomponent system.

EXPERIMENTAL SECTION

Samples. For the detailed synthesis process of thermal reversible Diels−Alder cross-linked polyurethane (DAPU), please refer to our recent work.[21] Generally, poly(tetramethylene ether glycol) (PTMEG) is first condensed with 4,4-methylene bis(phenylisocyanate (MDI) and then reacted with a chain extender *N*-(2,3-dihydroxypropyl) maleimide (DHPM), producing a linear polyurethane with DA reactive side-group, as shown in Figure 1a. A mixture of the linear polyurethane and different amounts of cross-linkers (1,6-hexamethylene-bis(2-furanylmethylcarbamate, FHF, Figure 1b) in dimethylacetamide (DMAc) solution was then cast on a PTFE plate. After removing the solvents at room temperature under vacuum followed by heating, the final cross-linked polyurethane (Figure 1c) sample is obtained, which is fully transparent, and mechanically very hard and tough. According to different mole ratios of furan to maleimide group (φ_c, proportional to the content of cross-linkers) from 0 to 1.0, the samples are denoted as DAPU0, DAPU25, DAPU50, DAPU75,

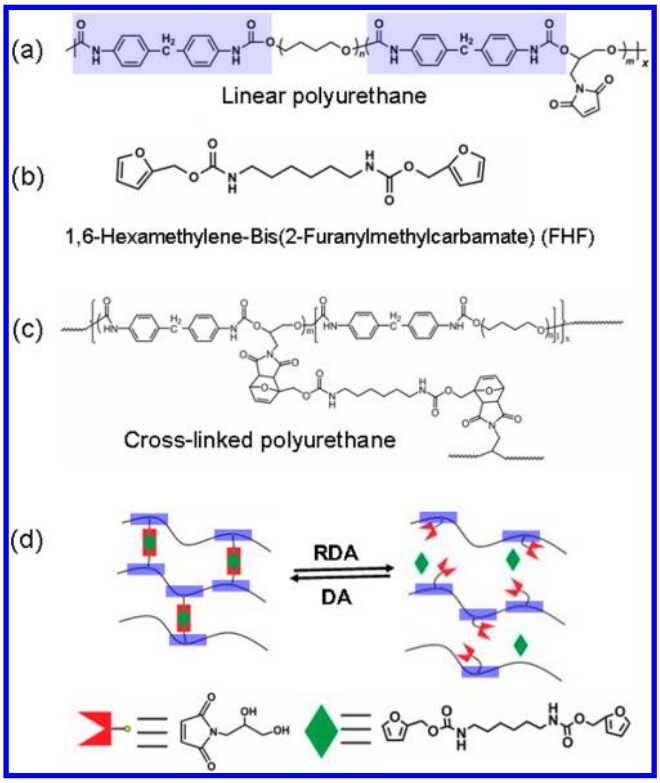

Figure 1. Molecular structures of (a) linear polyurethane, (b) cross-linker, FHF, and (c) the cross-linked polyurethane. (d) A schematic view of a reversible DA covalent cross-linked network. The hard segments are indicated in the light blue rectangle block in parts a and d.

dx.doi.org/10.1021/jp409893f | J. Phys. Chem. B 2014, 118, 1126−1137

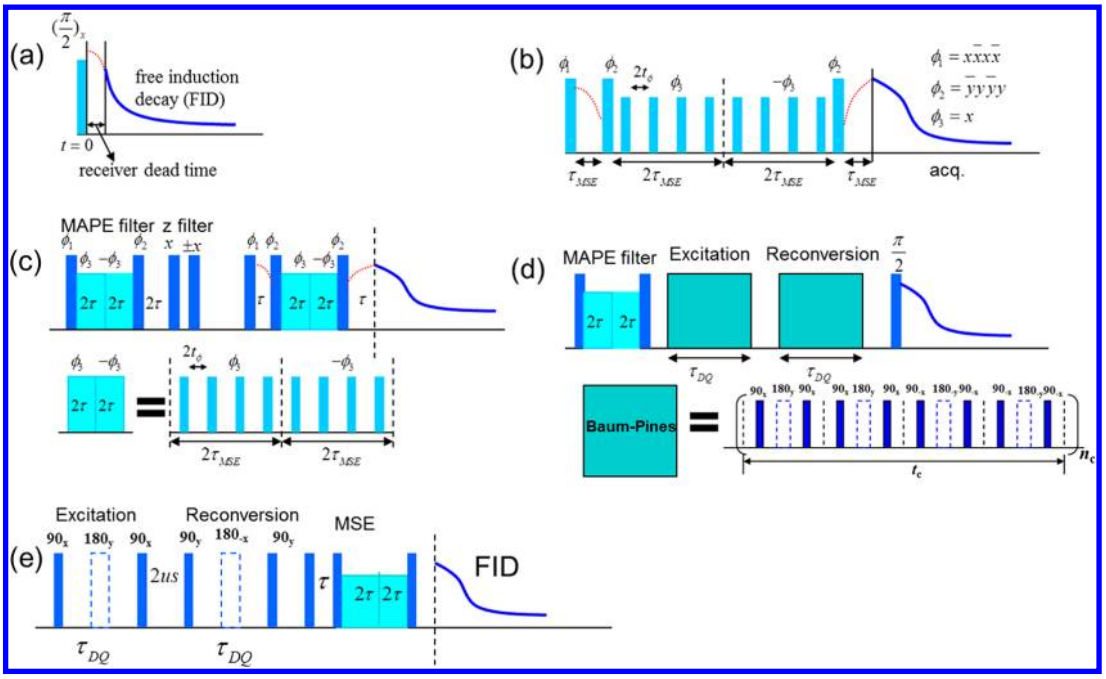

Figure 2. Pulse sequence in the low field spectrometer. Solid bars denote 90° pulses, while open bars denote 180° pulses. (a) Single pulse excitation experiment for detecting the free induction decay (FID) signals, where the initial part is missing due to the receiver dead time of the spectrometer. (b) Magic-sandwich echo (MSE) pulse sequence for refocusing the loss of rigid-phase signal due to the receiver dead time. (c) Magic and polarization echo (MAPE) filter for suppressing rigid-phase signals. A phase-cycle controlled magnetization inversion is applied before FID signals are recorded with MSE detection. (d) The Baum−Pines multiple-quantum experiment is preceded by a MAPE filter to remove the response of rigid/glassy polymer signals. (e) Three-pulse multiple-quantum experiments for investigation on rigid components. FID signals are also recorded with MSE detection in order to avoid the loss of rigid signals due to the receiver dead time.

and DAPU100, respectively, where φ_c is 0, 0.25, 0.50, 0.75, and 1, respectively. A schematic view of the reversible DA covalent cross-linked network is also shown in Figure 1d.

Low-Field ^{1}H NMR. The measurements were performed on a Bruker Minispec mq20 low-field spectrometer at 20 MHz proton resonance frequency. The sample temperature was controlled with a BVT3000 heater working with a flow of heated air. In order to avoid O_2-related sample degradation, the NMR tube (10 mm outer diameter) was first flushed with argon gas, and then flame-sealed. The Minispec has a typical $\pi/2$ pulse length of about 3 μs and a receiver dead time of about 13 μs.

Magic-Sandwich Echo Experiment. In a general way, the free induction decay (FID) of proton time-domain NMR signal is mainly governed by the widespread distribution of ^{1}H−^{1}H pair dipolar coupling interactions, which are dependent on the distances between spins as well as the internuclear orientations relative to the magnetic field. In the immobile glassy or crystalline polymers, proton spins at close distances will have strong dipolar coupling with each other, leading to a rapid decay generally less than 50 μs in the time domain,[33] and thus a broad peak in the frequency spectrum. On the contrary, for the protons experiencing fast segmental or subsegmental motions, the dipolar couplings will be averaged to a great extent, resulting in a long characteristic decay time, i.e., the apparent T_2 relaxation time, in the time domain on the order of milliseconds to seconds, and thus a narrow peak in the frequency spectrum. Therefore, the premise of the accurate quantification of each different component fraction is to get a fully well recorded FID signal. The conventional single pulse experiment will result in the missing of the initial part of FID due to the dead time problem of the Minispec receiver, as shown in Figure 2a. Therefore, a full dipolar time-reversed magic-sandwich echo (MSE) pulse sequence has to be utilized to tackle the above problem, as shown in Figure 2b.[34] The final echo time τ_{MSE} can be adapted to the receiver dead time by adjusting the finite phase switching time t_ϕ of the instrument, and thus to almost fully recover the FID and its shape, denoted as MSE-FID. This pulse sequence is also much more efficient than the conventionally used solid-echo, which fails to refocus multispin dipolar interactions.[35] The quantification of each different component fraction is achieved by fitting the MSE-FID signals utilizing a combination of modified exponentials, $e^{-(t/\tau)^b}$.[36] The decay signal of a rigid/glassy component generally could be fitted with a Gaussian function ($b = 2$) along with a very short characteristic time τ (20−40 μs), whereas an exponent $b \sim 1$ along with a long τ could well describe the decay behavior of potentially inhomogeneous mobile components. Intermediate dynamics are often reflected in apparent exponents between 2 and 1. Herein, the final fully refocused MSE-FID decay signal could be fitted with the following formula:

$$I(t) = f_r \exp(-(t/T_{2r})^2) + f_i \exp(-(t/T_{2i})^{n_i}) + f_m \exp(-(t/T_{2m})^{n_m}) \quad (1)$$

where $T_{2r} < T_{2i} < T_{2m}$.

Magic and Polarization Echo (MAPE) Filter Experiment. The MAPE sequence is a dipolar filter which consists of a $(\pi/2)_x$ pulse followed by a train of magic sandwiches, as shown in Figure 2c. In general, the T_2 filter has an efficiency proportional to T_2^{rigid}/T_2^{mobile} in selecting the transverse magnetization, while the MAPE filter has an efficiency increasing with the $6n$ power of this ratio in filtering out the rigid-phase signals,[37] where n means the number of magic sandwich pulses in the

dx.doi.org/10.1021/jp409893f | J. Phys. Chem. B 2014, 118, 1126−1137

MAPE filter, and will lead to a higher amplitude of the selected z-magnetization gradient compared to the multiple-pulse dipolar filters based on solid echoes.[38,39] In this sequence, the amplitude of selected z-magnetization gradient could be adjusted by changing the finite phase switching time t_ϕ similar to the MSE sequences. For preventing the possible loss of rigid signals due to the receiver dead time problem, a MSE sequence also procedes the formal FID acquisition.

Multiple-Quantum (MQ) NMR. ^{1}H MQ NMR is a very versatile, robust, and quantitative tool for investigating the structure and dynamics in polymer network or melts.[40] And for a complete account of the principle of MQ NMR as applied to polymers and soft materials, please refer to ref 40. In solids, the excitation of MQ signals relies on the presence of residual dipolar coupling (D_{res}) among protons, which vice versa renders MQ NMR as a sensitive probe for the determination of D_{res}. As D_{res} is determined by the proton−proton distances as well as the internuclear directions relative to the magnetic field, it could further provide information about the anisotropy of molecular motions caused by the polymer cross-linked network or entanglements.

Briefly spoken, there are two most common excitation schemes for higher-order spin coherences in static MQ experiments. One is the Baum−Pines sequence,[41] and the other is the so-called three-pulse sequence (90_x-τ-180_y-τ-90_x),[42] as shown in Figure 2d and e. The most important difference between the two DQ excitation schemes lies in the efficiency of exciting DQ signals of rigid/mobile components. The Baum−Pines sequence could produce a pure DQ Hamiltonian, and due to the limit of minimum sequence length, about 0.1 ms, its performance is more robust at long excitation time τ_{DQ}, making it able to deal with multiple-spin weak dipolar couplings found in rubber or melts far above the glass transition,[43,44] whereas the three-pulse sequence suffers from a severe limitation in refocusing multispin dipolar interactions but is more efficient when rather strong couplings are present due to the much shorter minimum excitation time, ∼10 μs. In this paper, both excitation schemes are utilized to study the microstructure and dynamics of soft and hard domains of polyurethane, respectively.

It is worth noting that the normalized DQ buildup curve obtained from three-pulse MQ NMR experiments could not completely eliminate the temperature-dependent relaxation effect due to its failure to produce a pure DQ Hamiltonian. However, at short excitation time, the relaxation effect could be well ignored, as reflected in a plateau of 0.5 in the normalized DQ buildup curve. For the investigation of soft segments using the Baum−Pines sequence, the interference of rigid signals has to be filtered utilizing a MAPE filter, as shown in Figure 2d.

The detailed analysis of MQ experiment data has been well described in the literature,[43,45−47] and we are not planning to go into detail here. For a very homogeneous system, the normalized DQ intensity can be calculated and analyzed according to eq 2[45]

$$I_{nDQ}(\tau_{DQ}, D_{res}) = 0.5[1 - \exp\{-(0.378 D_{res}\tau_{DQ})^{1.5}\} \cos(0.583 D_{res}\tau_{DQ})] \quad (2)$$

where D_{res} is the apparent residual dipolar coupling. However, in most cases, a Gaussian or gamma distribution of D_{res} will be assumed due to the presence of system heterogeneity, and then, the final total DQ buildup is calculated as a numerical finite-step integral according to

$$I_{nDQ}(\tau_{DQ}) = \int P(D_{res}) I_{DQ}(\tau_{DQ}, D_{res})\, dD_{res} \quad (3)$$

using eq 2 as the $I_{DQ}(\tau_{DQ}, D_{res})$ Kernel function.

However, please note that the above formula could only be directly utilized for the analysis of Baum−Pines MQ NMR results. The free dipolar coupling evolution during τ_{DQ} for the three-pulse sequence features a prefactor of 3/2 compared to the Baum−Pines sequences.[40] Therefore, for the three-pulse sequence, the time axis (τ_{DQ}) of the DQ and MQ curves has to be multiplied by 3/2 in order to make the above formula applicable for fitting, or make the obtained D_{res} divided by 3/2 return the accurate value of D_{res} if the above formulas are directly used for three-pulse DQ NMR result analysis.

High-Field ^{13}C NMR. 2D ^{1}H−^{13}C wide-line separation (WISE) NMR[48,49] and static proton 12-pulse dipolar filter spin diffusion[50,51] experiments were performed on a Varian Infinitplus-400 wide-bore (89 mm) spectrometer operating at a ^{1}H frequency of 399.7 MHz and a ^{13}C frequency of 100.5 MHz. WISE experiment was performed using a conventional 5 mm double-resonance HX CP/MAS NMR probe at a magic angle spinning (MAS) frequency of 4.5 kHz controlled with a MAS speed controller. The Lee−Goldburg (LG) decoupling pulses were adopted during the cross-polarization (CP) period to avoid proton spin diffusion, and the CP contact time was 0.5 ms. The ^{1}H effective field strength during LG was about 78.9 kHz with a resonance offset of 45.0 kHz. The TOSS (total suppression of sidebands)[52] sequence was also used before signal acquisition to suppress the spinning sidebands. Heteronuclear decoupling during the acquisition period was achieved by SPINAL-64 irradiation.[53] The length of the 90° radiofrequency pulse was about 3 μs on both the ^{1}H and ^{13}C channels. For the static proton spin diffusion experiment, a 4 mm double-resonance HX CP/MAS NMR probe was used, and the length of the ^{1}H 90° radiofrequency pulse was about 2.5 μs. The dipolar filter strength was determined by the 12-pulse dipolar filter cycles as well as the 90° interphase spacing. The ^{13}C and ^{1}H chemical shifts were referenced to external HMB (hexamethylbenzene, ^{13}C δ_{iso} = 17.3 ppm for CH_3 group) and TMS (^{1}H, δ_{iso} = 0 ppm), respectively.

RESULTS AND DISCUSSION

Composition Dynamics and Microphase-Separated Structures. As is known, the segmented polyurethane will microphase-separate due to the incompatibility between the hard and soft segments, which is the general characteristic of segmented polyurethane. The understanding on the micro-domain structure and its relevant composition dynamics is of significant importance for revealing the structure−property relationship of materials, as well as improving the design of novel high-performance materials. The mobility difference between different components also facilitates our analysis on the heterogeneous structures, and distinct polymer mobilities can be distinguished utilizing T_2 relaxometry experiments with a benchtop low-field NMR spectrometer. Low-field proton NMR has been a well-established method in recent years for investigating polymer composition,[54] the topological constraints induced by cross-linking or entanglements and defects,[43,46,55] and the thermodynamics of polymer network.[56,57] Herein, we will first extract quantitative information about the compositions of DAPUs with the T_2 relaxometry method as well as the microphase separation with a combination of 2D WISE NMR and SAXS. As shown in

dx.doi.org/10.1021/jp409893f | J. Phys. Chem. B 2014, 118, 1126−1137

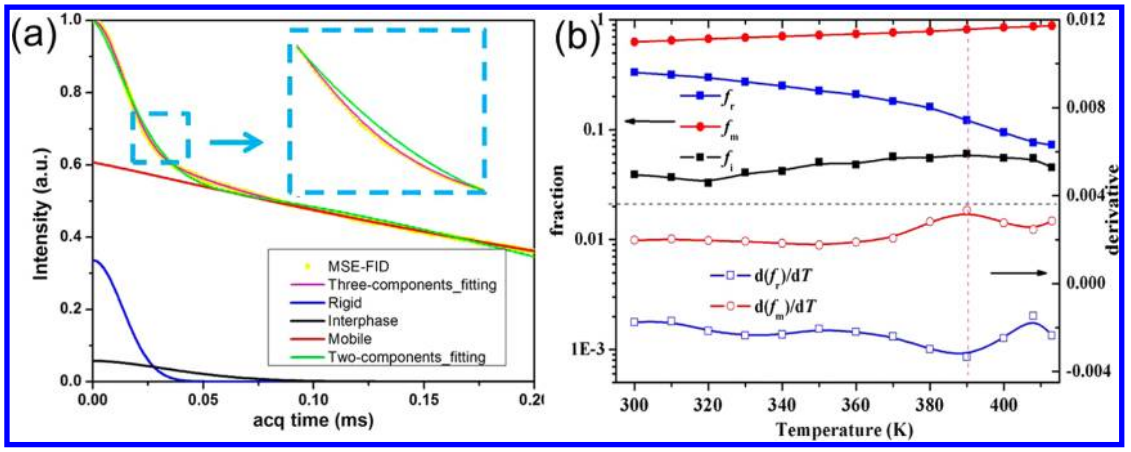

Figure 3. (a) The MSE-FID signal of DAPU100 at room temperature as well as the different component signals resulted from the fitting. The two-component fitting result is poor, as reflected from the indicated blue part in dashed lines. (b) The fraction of rigid (f_r), interphase (f_i), and mobile component (f_m) in DAPU100 as a function of temperature and the corresponding derivative curve to temperature. The solid lines are only shown as guidelines to the eyes.

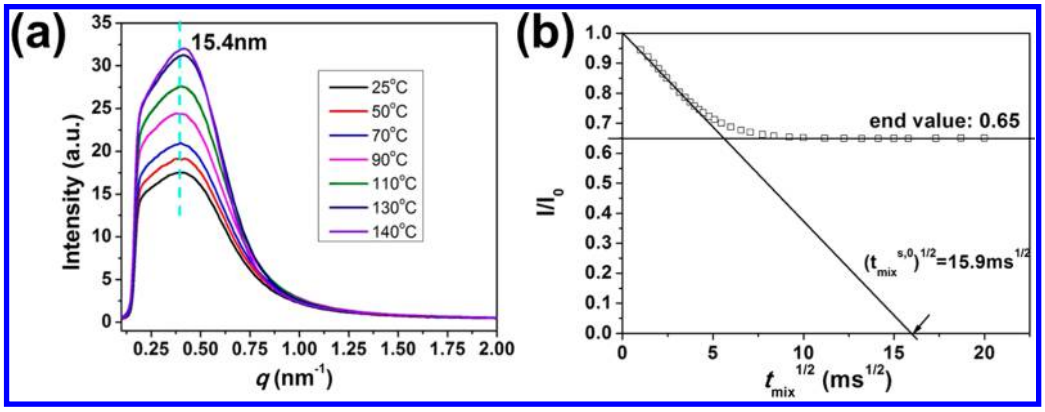

Figure 4. (a) SAXS scattering pattern at different temperatures for DAPU100. (b) Proton spin diffusion curve of DAPU100 at room temperature for the determination of domain size and interphase thickness. The 12-pulse dipolar filter cycle is set as one, and the 90° interpulse spacing is 15 μs. The interfacial spin diffusion coefficient is assumed as the average of spin diffusion coefficients of mobile and hard segments, both of which are determined from the line width of proton wide-line signals obtained from 2D WISE experiments.

Figure 3a, the MSE-FID decay signal could be well fitted with eq 1. It is worth noting that the MSE-FID could not be fitted well with only two components, i.e., two stretched exponential functions, which means that there are at least three different components. On the basis of the microphase-separated structure, it is reasonably assumed that an interphase is present between the hard and soft domains, which may come from the partial mixing of PTMEG soft segments with hard segments containing MDI (and/or BDO). We cut the MSE-FID signal at an acquisition time of 200 μs, as the magnetic field inhomogeneity begins to play an important role at longer acquisition time, which hence will result in the signal decay and may become dominating. The reliability of our fitting method with eq 1 could be further supported by the smooth variation of rigid/mobile fraction with increasing temperature, as shown in Figure 3b. Also, please note that the interphase fraction is always very small, about 5% throughout all temperatures. On the one hand, the small fraction of interphase indicates that the polyurethane is well phase-separated. On the other hand, the interphase changes little with temperature, which to a large degree means that the microstructure is stable. This result is proven by the SAXS experiments shown in Figure 4, where the length of microdomain periodicity did not change with increasing temperature. Furthermore, it is also interesting to note that there is an obvious turning point for the rigid fraction curve at around T = 390 K, corresponding well to the inflection point of the curve of fraction derivative to temperature. Such a turn mainly results from the occurrence of RDA reactions at high temperatures, resulting in the disassociation of the cross-linked network, as also reflected in the DSC experiments.[21] After the disassociation of the DA cross-linkages, the cross-linkers become very mobile, and may enhance the mobility of hard segments as a plasticizer. Therefore, by observing the variation of rigid fraction with increasing temperature, the RDA reaction temperature can be determined in situ.

The microphase separation structure and thermal stability of DAPU100 can be further examined with SAXS experiments, as shown in Figure 4a. A strong peak is observed at low q for all temperatures, indicating the presence of microdomain periodicity and microphase separation in the material. The length of microdomain periodicity could be determined from the peak position in the SAXS curves according to the Bragg equation $d = \lambda/(2 \sin \theta)$, where $\sin \theta = q\lambda/4$. Proton dipolar filter spin diffusion experiment is further performed to determine the domain size and interphase thickness. As shown in Figure 4b, the domain size and interphase thickness are estimated to be 16.1 and 3.5 nm, respectively and the calculated long period is about 20.1 nm, which are obtained using our calculation

dx.doi.org/10.1021/jp409893f | J. Phys. Chem. B 2014, 118, 1126−1137

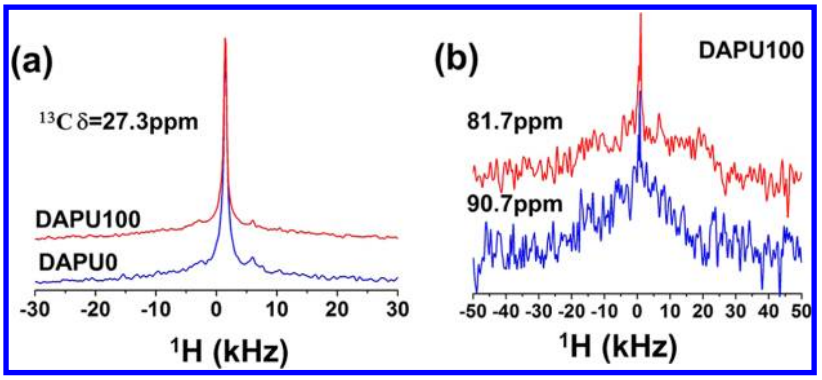

Figure 5. (a) Slice at 27.3 ppm (ascribed to PTMEG signals) in the ^{13}C dimension for DAPU100 and DAPU0. (b) Slice at 81.7 and 90.7 ppm (both ascribed to DA cross-linkage signals) in the ^{13}C dimension for the DAPU100 sample.

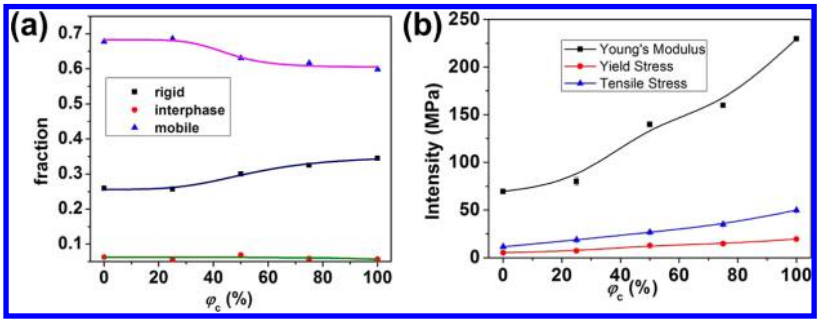

Figure 6. (a) The fraction of rigid, mobile, and interphase as a function of the cross-linker content at room temperature. (b) The Young's modulus, yield stress, and tensile stress as a function of the cross-linker content. Those data of mechanical properties are obtained directly from our recent work for comparison, where the tensile and yield stress are measured at 300 and 14% strain, respectively.[21]

procedure published previously.[51] The result is slightly larger than what we got from SAXS experiments but still reasonable, which may result from the heterogeneous distribution of domain sizes and morphology in DAPU100 as well as the mismatch between the real morphology and the model we utilized in the calculation procedure.[39,51] It is noteworthy that, with increasing temperature, the peak position and peak width in SAXS curves change little, whereas the peak intensity grows obviously. The constant peak position indicates a constant length of microphase separation periodicity which could be ascribed to the thermal stability of the microstructures in polyurethane. The micro-order periodicity has not been destroyed at all by the high temperature, even though the cross-linking is dissociated by the RDA reaction at high temperature above 110 °C.[21]

The thermal stability of the DAPU microstructure also could be demonstrated from the variation of SAXS peak intensity and peak width with temperature. On the one hand, generally speaking, the increased molecular mobility at high temperature will induce severe composition fluctuation,[58] which will make the structure become more heterogeneous, resulting in a larger peak width in SAXS curves. At the extreme case without decomposition, the molecules will have so large mobility that the microphase-separated structure could not be stabilized any more through the intermolecular interactions. However, for the DAPU100, the peak width changes very little with increasing temperature, indicating a weak influence of composition fluctuation on the microphase structure. This might be ascribed to the widespread hydrogen bonding network among hard segments.

On the other hand, in most cases, an elevated temperature will weaken the microphase separation due to the increased molecular mobility and entropic interactions. The peak intensity in the SAXS curves will decrease with microphase separation weakening; hence, a complete microphase mixing is achieved when the peak completely disappears at a specific temperature which is defined as the order−disorder transition temperature.[59] However, for the DAPU100 sample, an obvious increase of peak intensity can be observed when the temperature is increased, which indicates an enhanced microphase separation. In another way, the microstructure is becoming more and more ordered, which may result from the increased enthalpic interactions of mutual repulsion between hard and soft segments with increasing temperature. Both the hard and soft segments tend to form their own domain. Thus, at high temperatures, to a large degree, the enthalpic interaction still overwhelms the entropy for our DAPU100 sample, resulting in a more ordered microphase structure. It is worth noting that such enhanced microphase separation with increasing temperature does not reflect well in the T_2 relaxometry data shown in Figure 3, where the interphase is imagined to decrease obviously upon heating. However, as shown in Figure 3b, the fraction of interphase is rather small, about 5% according to our MSE-FID fitting results, whereas the systematic error associated with ambiguity of the fitting procedure is also estimated to be around 5%, rendering the variation of interphase fraction with temperatures ambiguous.

The microphase-separated structure and heterogeneous dynamics can be further confirmed by the 2D ^{1}H−^{13}C wide-line separation (WISE) NMR experiments, as shown in Figure 5. WISE experiments are widely utilized to characterize polymers with heterogeneous dynamics and multiphase structures that include hard and soft components. Components are distinguished by the ^{1}H wide-line spectrum (F1 dimension),

dx.doi.org/10.1021/jp409893f | J. Phys. Chem. B 2014, 118, 1126−1137

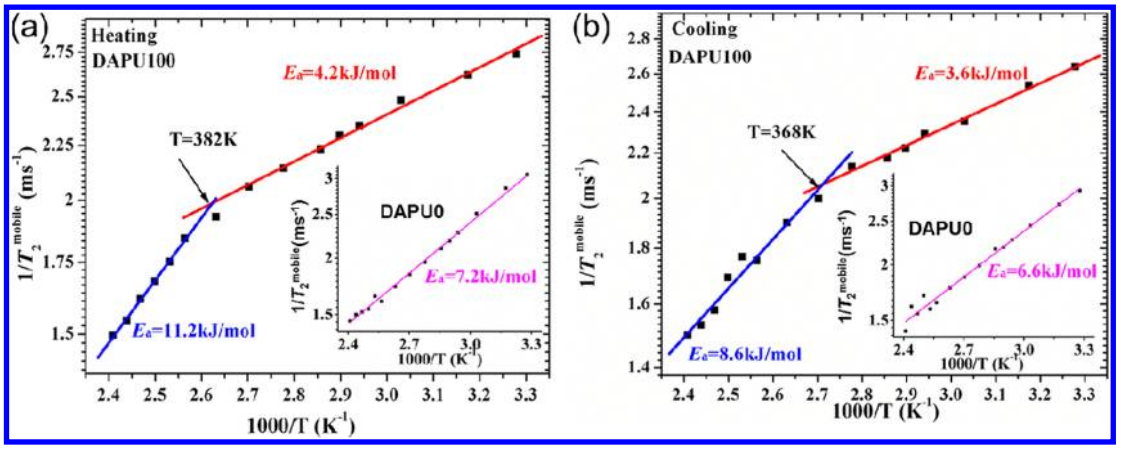

Figure 7. The inverse apparent spin−spin relaxation time of the mobile component $1/T_2^{mobile}$ as a function of the temperature during heating (a) and cooling (b) processes, where the temperature of RDA and DA reactions could be determined. The solid lines are the Arrhenius fits over temperatures, yielding the corresponding apparent activation energy for the motion of segments.

broad if rigid and narrow if mobile, whereas the corresponding ^{13}C chemical shifts on F2 dimension indicate the chemical compositions. The solid-state ^{13}C CP/MAS spectrum of DAPU100 was shown in our recent work,[21] where the signal at 27.3 ppm is ascribed to PTMEG, while both signals at 81.7 and 90.7 ppm are ascribed to the DA cross-linkages. It was clearly shown that a strong narrow peak is in the center in Figure 5a, indicating a high mobility for PTMEG due to its much lower glass transition temperature, around −75 °C. In addition, a small broad bottom signal could also be observed, indicating a very small fraction of PTMEG chains suffers from restriction in mobility due to their incorporation into the hard domain, forming an interphase. The opposite situation is found in the proton wide-line spectra of the cross-linker, sliced at 81.7 and 90.7 ppm in the ^{13}C dimension for the DAPU100 sample, as shown in Figure 5b. A strong broad signal in the bottom implies that most of the cross-linkers are in the hard domain, while the narrow sharp peak in the center demonstrates the presence of a small amount of cross-linker chains in the interphase.

As was shown in our recent paper,[21] the mechanical properties and long period of the ordered domain in DAPU could be adjusted through changing the content of cross-linkers. Therefore, it is of importance to understand the role of cross-linkers in the DAPU samples. T_2 relaxometry is also used to determine the fraction of each different component as a function of the cross-linker content, as shown in Figure 6. With increasing cross-linker amount, the fraction of rigid components increases, whereas the mobile fraction decreases, which indicates that the cross-linker mainly contributes to the hard domain of DAPU. Herein, on the basis of the molecular structure, it can be deduced that the flexible polyether (PTMEG) forms the mobile domain, whereas the MDI, including the cross-linker, forms the hard domain. Indeed, according to our molecular design idea of DAPUs, the cross-linker, which contains urethane bonds, is specially selected to promote miscibility with hard segments and to further increase the H-bonding density in the hard domain, and thus to enhance the mechanical properties. A strong hydrogen bonding interaction between hard segments and cross-linkers will indirectly restrain the enthalpic interaction between hard and soft segments, enhancing the phase separation of soft segments from the hard domain, and thus to form a small interphase, as reflected from the small interphase size obtained for spin diffusion NMR experiments in Figure 4b. It is worth noting that Young's modulus, yield, and tensile stress all increase with increasing cross-linker content, as shown in Figure 6b, corresponding well to the variation tendency of the fraction of rigid components with the addition of cross-linkers, as shown in Figure 6a. It is easy to understand such a correspondence considering that the cross-linker is mainly involved in forming the hard domain, whereas the stiffness and strength increase with hard segment content.[25,26]

Overall, the microdomain structure, resulting from the microphase separation between soft and hard segments, is very stable even at high temperatures beyond the dissociation of DA cross-linkages, and the microphase separation will also be enhanced with increasing temperature. Furthermore, the incorporation of DA cross-linkers containing urethane bonds mainly contributes to the hard domain due to the strong hydrogen bonding interactions and DA reaction between the cross-linker and maleimide pendant groups of the chain extender on hard segments, and thus results in the enhancement of microphase separation as well as the growth of the fraction of rigid components. Those microscopic structures also correspond well with the enhancement of stress and modulus with increasing cross-linker contents.

In Situ Monitoring of Reversible Cross-Linking Associated with DA and RDA Reactions. Although both liquid and solid state NMR have been reported to be used to detect the (R)DA reaction in reversible cross-linked polymers,[10,16,20,60] the in situ monitoring of (R)DA reaction still remains a great challenge. As shown in our recent work,[21] the DA reactions happen so fast that even quenching the sample from a high temperature could not stop the occurrence of DA reaction in DAPUs. And that is why in situ solid state NMR has to be utilized to prove the presence of DA and RDA reactions. However, it would be better if we could identify the actual temperature for the reactions, which will benefit us to monitor the reactions, and thus to prepare better products. Although ^{13}C NMR spectroscopy provides a higher resolution, as shown in previous work,[10,21,60] it often requires longer experimental time due to the poor sensitivity arising from the low abundance of ^{13}C spins and gyromagnetic ratio. Therefore, ^{1}H spectroscopy would be a good alternative due to its high sensitivity if it could be utilized for the detection of (R)DA reactions. Until now, few NMR methods have been reported to effectively characterize the connection and disconnection of the cross-

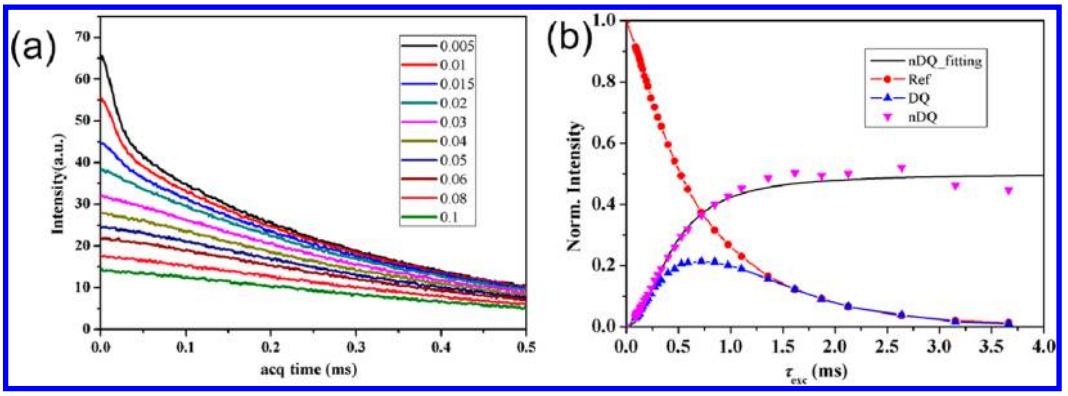

Figure 8. (a) Adjustment of the MAPE filter. As the filter time τ is increased in the MAPE filter, the rigid signal in the MSE-FID decreased. In this paper, τ was set as 0.08 ms. (b) DQ buildup curve and reference signal decay of the soft segments in DAPU100 at room temperature. The normalized DQ buildup signal is fitted with eq 3 assuming a gamma distribution for D_{res}, yielding an averaged residual dipolar coupling (D_{avg}) around 600 Hz, and other solid lines are only used as a guideline for the eyes.

linking network associated with DA and RDA reactions in reversible cross-linked polymers. Here, the ^{1}H inverse decay time constant of the mobile component, $1/T_2^{mobile}$, obtained from the MSE-FID fitting, as a function of temperature could be used to address the above issue and identify the temperature of DA and RDA reactions, as shown in Figure 7. This method is quite fast and effective as the acquisition of MSE-FID often only takes one or several minutes.

In the motion narrowing limit,[61] the temperature dependence of spin−spin relaxation time could be utilized as a probe of proton mobility, which is argued to result from the proton hopping following an Arrhenius relation.[62]

$$\frac{1}{T_2} \approx \tau_c = \tau_\infty \exp\left(\frac{E_\alpha}{RT}\right) \quad (4)$$

Therefore, the activation energy could also be obtained from the temperature-dependent $1/T_2^{mobile}$.

We did not choose the apparent T_2 relaxation time of the rigid or interphase component, because, in the rigid limit, T_2^{rigid} is always around 20 μs without significant change, and in the intermediate state, the intermediate fraction is very small, causing the variation of T_2^{inter} to be ambiguous. Only the apparent T_2^{mobile} has a broad range, and is more sensitive to the mobility variation resulting from the temperature variation or (R)DA reactions. As shown in Figure 7a, upon heating, there is an obvious turning point for $1/T_2^{mobile}$ of DAPU100 at about T = 382 K, whereas there is none for the DAPU0 sample upon heating due to the absence of RDA reaction. Therefore, the RDA reaction actually occurs at around 382 K, corresponding well with the actual experimental temperature.[21] Upon cooling, as shown in Figure 7b, the DA reaction actually occurs at around 368 K. The activation energies for the motions of soft segments before and after the DA/RDA turning point are obtained through the Arrhenius fitting of eq 4. For the DAPU0 sample, the activation energy is almost the same for the heating and cooling processes, both around 7.0 kJ/mol, indicating the absence of (R)DA reactions. In contrast, for the DAPU100, an obvious difference in activation energy is observed at high temperatures for the heating and cooling process, which could be ascribed to the disassociation of hydrogen bonds between cross-linker and hard segments as well as RDA reaction at high temperatures. Therefore, before the DA reaction in the cooling process, the molecular motions of soft segments are enhanced by the presence of cross-linkers, resulting in smaller activation energy. When the DA reaction is finished, the activation energy for the soft segment is almost the same as that in the heating process, indicating an almost complete reconstruction of cross-linking network. It is worth noting that the activation energy for DAPU0 is larger than that for DAPU100 in the low temperature region upon cooling and heating processes. As mentioned above, for DAPU100, the cross-linking between the cross-linker and hard segments actually enhances the phase separation, resulting in weaker restraint of the hard domain on the soft segments. Therefore, the activation energy for the motion of soft segment in DAPU100 is smaller in the low temperature region compared to DAPU0 without any cross-linkers. In contrast, the activation energy for DAPU0 is smaller than that for DAPU100 in the high temperature region, either in the cooling or heating process. Because the furan cross-linkers, which are considered as hard segments at low temperatures, have become quite mobile at high temperatures due to the disassociation of DA cross-linking, it will increase the fraction of mobile components, and thus result in higher activation energies for the mobile components. This result also demonstrates that the activation energy of the mobile component is a sensitive probe to detect the DA(RDA) reactions in such systems.

Heterogeneous Structures and Dynamics Revealed by ^{1}H MQ NMR. Proton MQ NMR has been well established and proved to be a good method for investigating the heterogeneous structures and dynamics of polymeric materials.[40,43,44,57] Compared to the T_2 relaxometry method, MQ NMR could further provide detailed information about the heterogeneous network structures of polyurethane and its related anisotropic mobility. As is known, the DA cross-linking occurs between the hard segments and the cross-linker FHF, containing urethane bonds. The hydrogen bonding network is more widespread due to the incorporation of FHF into hard domains.[21] To a great extent, the strong hydrogen bonding interactions directly improve the toughness and modulus of DAPU samples. Besides, it would also be interesting to understand whether the structure and dynamics of soft segments will be affected by the incorporation of DA cross-linkers. Herein, we utilize proton DQ NMR experiments to investigate the structures and dynamics of the mobile and rigid domains. As the DAPU is a multiphase system, the signals of rigid segments have to be filtered out so that we are able to access the mobile signals. In this way, the MAPE dipolar filter is an efficient method for filtering the rigid signal and keeping the

dx.doi.org/10.1021/jp409893f | J. Phys. Chem. B 2014, 118, 1126−1137

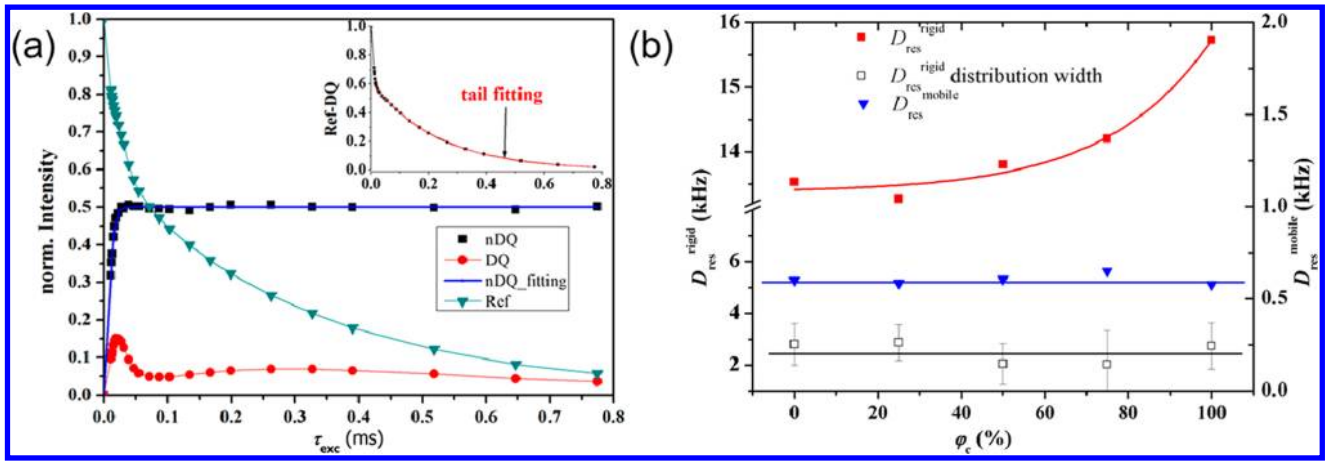

Figure 9. (a) DQ buildup curve and reference signal decay of the hard segments in DAPU100 at room temperature. The nDQ curves were fitting with eq 3 assuming a Gaussian distribution of D_{res}, and other solid lines are only used as guidelines for the eyes. (b) The apparent D_{res} of rigid and mobile components as well as the distribution width of D_{res}^{rigid} as a function of the content of cross-linkers. The solid lines are used as guidelines for the eyes.

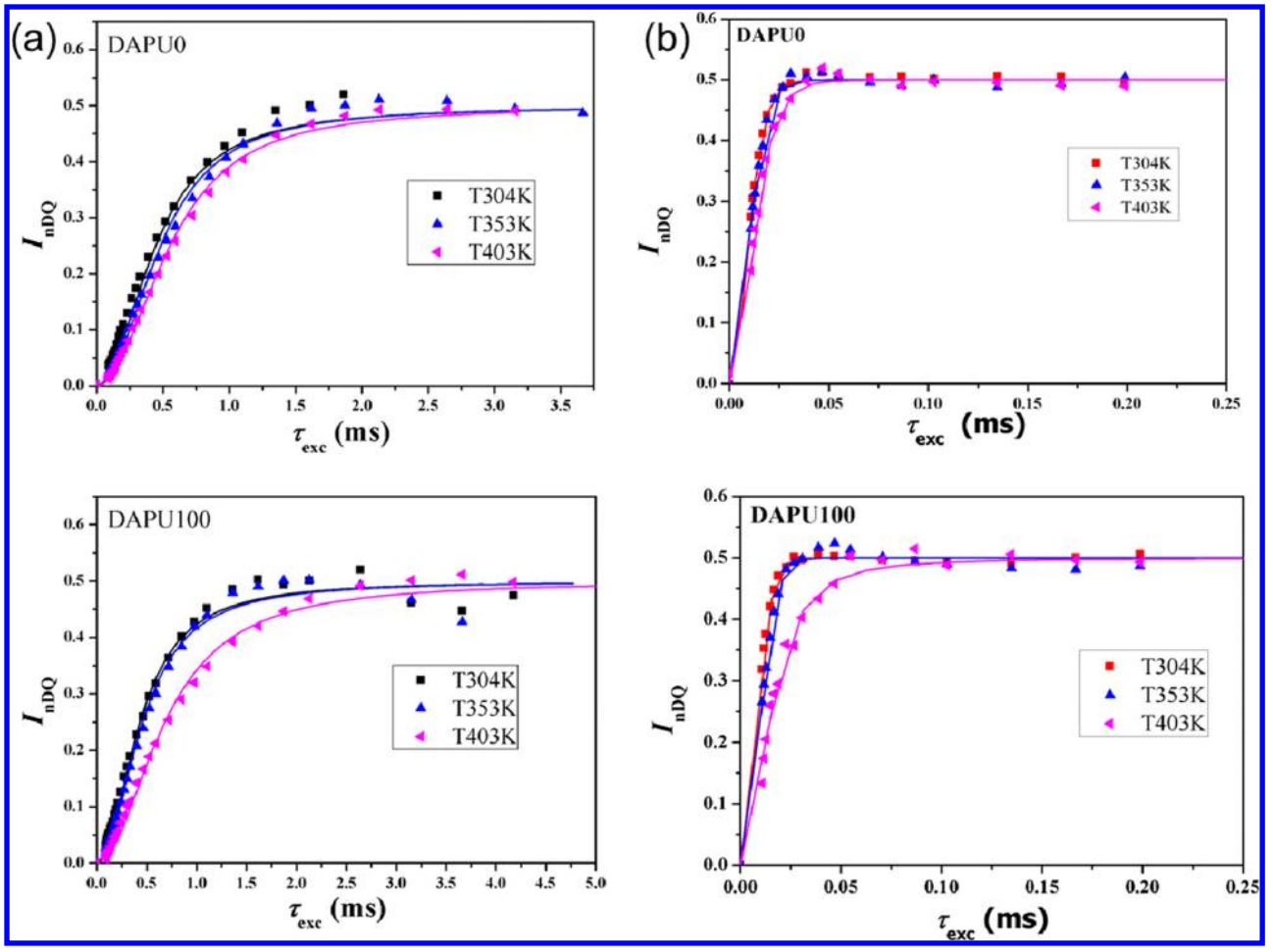

Figure 10. The normalized DQ buildup curve of soft (a) and hard (b) domains of DAPU0 and DAPU100 at different temperatures obtained from Baum–Pines and three-pulse MQ NMR experiments, respectively. The fitting results of the buildup curve are shown in solid lines.

mobile one. As shown in Figure 8a, with increasing filter strength, i.e., increasing τ, the solid-like response (rigid signal) within a rather short acquisition time decreases, while most of the mobile signals are retained, reflecting as a long decay in the FID signals. In order to obtain pure soft segment signals, the filter time τ is set as 0.08 ms in the MAPE filter preceding the Baum–Pines DQ NMR sequences, as shown in Figure 2d. The normalized DQ buildup signal in Figure 8b comes from the entanglement of soft segments, because the molecular weight of DAPU100 is around 170 kg/mol,[21] and the cross-linking occurs among hard segments. It is interesting to know that it is not necessary to subtract the tail from the sum intensity signal in

dx.doi.org/10.1021/jp409893f | J. Phys. Chem. B 2014, 118, 1126–1137

order to obtain the plateau of 0.5 in the normalized DQ curve, which means that there are not defects, such as loops or dangling chains, in the soft domain. The tight entanglement structure of soft segments, to a large degree, contributes to the toughness of the polyurethane. Furthermore, we obtain almost the same normalized DQ buildup curves for DAPU samples with different amounts of cross-linkers, all yielding a residual dipolar coupling (D_{res}) around 600 Hz, as shown in Figure 9b. Therefore, the incorporation of cross-linkages in the polyurethane does not have any influence on the entanglement structure of soft domains. However, it is interesting to note that, with increasing cross-linker content, the toughness of polyurethane increases linearly, as shown in the Supporting Information of our previous work.[21] Therefore, the soft domain structure does not contribute to the increase of the toughness, which indicates that the enhancement of toughness may mainly come from H-bonding aggregating clusters between cross-linkers and hard segments.

For accessing the structures and dynamics of the hard domains, another pulse sequence has to be used for excitation and reconversion of DQ signals. The three-pulse sequence in Figure 2e is efficient in exciting the DQ signals of extremely rigid components due to the short excitation/reconversion period. However, as the dipolar time reversal is not possible with the three-pulse sequence,[40] it will suffer from a multispin relaxation effect at longer excitation/reconversion time. Therefore, the three-pulse sequence could only be utilized to investigate the rigid components adopting short excitation/reconversion time under which condition the multispin relaxation effect is reduced to minimum and negligible. As shown in Figure 9a, we are able to obtain a typical normalized DQ buildup curve for DAPU100. It reaches the expected theoretical plateau of 50% of the total intensity, representing a good quality-control criterion of the reliability of the tail fitting. Here, the tail takes up around 70% of the whole intensity, which indicates the presence of defects, such as dangling chains. However, the presence of stable dangling chains along the cross-linked backbone in a polyurethane cross-linked network may enhance its thermal self-repairing ability due to its greater mobility.[63,64] As the cross-linking occurs between the hard segment and the cross-linkers, it would be important to know the influence of cross-linkers on the structure and dynamics of hard segments. As shown in Figure 9b, with increasing cross-linker content, the apparent D_{res}^{rigid} increases. The increase is obvious, and generally, it is caused by the formation of a widespread strong hydrogen bonding network between the cross-linker and the hard segments, resulting in a stronger restraint on the mobility of hard segment as well as a significant improvement in modulus and strength,[21] as reflected in Figure 5b. It is also worth noting that the distribution width of D_{res} does not change much at different amounts of cross-linkers, which means that the incorporation of cross-linkers does not result in a large variation of the original microstructure of hard domains.

Herein, ^{1}H MQ NMR again proves itself as a powerful method for investigating the heterogeneous structure and dynamics of a multicomponent system. Indeed, the disassociation of cross-linkages could also be further demonstrated by the temperature-dependent proton normalized DQ buildup curves, as shown in Figure 10. Baum−Pines and three-pulse sequences are utilized to obtain the structure information of mobile and rigid components, respectively. For DAPU0, the temperature does not have any obvious influence on the normalized DQ buildup curves, indicating a stable entangled structure with constant residual dipolar couplings. However, for the DAPU100, at high temperatures (T = 403 K), the normalized DQ signals increase much more slowly than those at lower temperatures (T = 353 and 304 K), indicating smaller residual dipolar couplings. Without the disassociation of cross-linkages at T = 353 and 304 K, the normalized DQ buildup curves are exactly the same, indicating the similar structure and molecular mobility. However, due to the disassociation of cross-linkages at T = 403 K, the cross-linkers play the role of plasticizers to enhance the mobility of both soft and hard segments, resulting in weaker motional anisotropy of chainlike structures, and thus resulting in a slower buildup rate for the DQ signals. Therefore, the occurrence of disconnection associated with RDA reaction at high temperature can be well proved by the proton MQ NMR experiments.

CONCLUSION

In summary, we present a systematic investigation of the heterogeneous phase-separated structure and dynamics of a novel thermally reversible cross-linked polyurethane. Utilizing a benchtop low-field NMR spectrometer, proton T_2 relaxometry and MQ NMR experiments are performed, respectively. Through fitting on the fully refocused MSE-FID signals, the fraction of rigid, interphase, and mobile components are determined as well as the corresponding apparent spin−spin relaxation time T_2, where the occurrence of RDA reactions could be detected from the variation of component fractions as a function of temperature. The effects of temperatures and cross-linkers on the structures and dynamics are also discussed in detail, where the increase of temperature and incorporation of cross-linkers both enhance the microphase separation. Also, DAPUs remain thermal-stable even at a high temperature beyond the disassociation of the cross-linkages, rendering our polyurethanes of potential for applications at high temperatures. Furthermore, temperature-dependent T_2 relaxometry is first utilized to monitor in situ the reversible cross-linking associated with DA and RDA reactions, where the actual temperature of the reactions is determined as well as the activation energy of the motions of soft segments. The occurrence of disassociation of cross-linkages is also demonstrated with the temperature-dependent normalized DQ buildup curves. Finally, the heterogeneous structure and dynamics are both investigated with MQ NMR, where the incorporation of cross-linkers does not change the original structure of polyurethane but instead increases the modulus, toughness, and strength due to the formation of a widespread hydrogen-bonding network between cross-linkers and hard segments. All the results obtained from T_2 relaxometry and MQ NMR experiments correspond well with the mechanical data in our recent work. In short, our study on the microstructure and dynamics of polyurethane may serve as an example of understanding the macroscopic mechanical properties of polyurethane at a molecular level, and thus to enhance the design of new advanced polyurethane materials. It is also well demonstrated that proton T_2 relaxometry combined with MQ NMR is a good method to study the microstructure and dynamics of a multiphase system.

AUTHOR INFORMATION

Corresponding Authors

*E-mail: spclbh@nankai.edu.cn (P.S.). Phone: 086-022-2350-8171.

*E-mail: baohui@nankai.edu.cn (B.L.). Phone: 086-022-2350-8171.

Notes

The authors declare no competing financial interest.

■ ACKNOWLEDGMENTS

We thank Prof. Kay Saalwächter for providing the pulse programs on the minispec. Prof. Xiaoliang Wang and Dr. Yang Liu from Nanjing University are also acknowledged for the SAXS measurements. We are grateful for financial support by the National Science Fund for Distinguished Young Scholars (20825416) and the National Natural Science Foundation of China (21174072), 973 program (2012CB821503), PCSIRT (IRT1257), and the 111 Project (B12015).

■ REFERENCES

(1) Rowan, S. J.; Cantrill, S. J.; Cousins, G. R. L.; Sanders, J. K. M.; Stoddart, J. F. Dynamic Covalent Chemistry. *Angew. Chem., Int. Ed.* **2002**, *41*, 898−952.

(2) Corbett, P. T.; Leclaire, J.; Vial, L.; West, K. R.; Wietor, J. L.; Sanders, J. K. M.; Otto, S. Dynamic Combinatorial Chemistry. *Chem. Rev.* **2006**, *106*, 3652−3711.

(3) Maeda, T.; Otsuka, H.; Takahara, A. Dynamic Covalent Polymers: Reorganizable Polymers with Dynamic Covalent Bonds. *Prog. Polym. Sci.* **2009**, *34*, 581−604.

(4) Lehn, J. M. From Supramolecular Chemistry Towards Constitutional Dynamic Chemistry and Adaptive Chemistry. *Chem. Soc. Rev.* **2007**, *36*, 151−160.

(5) Wojtecki, R. J.; Meador, M. A.; Rowan, S. J. Using the Dynamic Bond to Access Macroscopically Responsive Structurally Dynamic Polymers. *Nat. Mater.* **2011**, *10*, 14−27.

(6) Boul, P. J.; Reutenauer, P.; Lehn, J.-M. Reversible Diels−Alder Reactions for the Generation of Dynamic Combinatorial Libraries. *Org. Lett.* **2004**, *7*, 15−18.

(7) Sauer, J.; Sustmann, R. Mechanistic Aspects of Diels-Alder Reactions: A Critical Survey. *Angew. Chem., Int. Ed.* **1980**, *19*, 779−807.

(8) Kwart, H.; King, K. The Reverse Diels-Alder or Retrodiene Reaction. *Chem. Rev.* **1968**, *68*, 415−447.

(9) Adzima, B. J.; Aguirre, H. A.; Kloxin, C. J.; Scott, T. F.; Bowman, C. N. Rheological and Chemical Analysis of Reverse Gelation in a Covalently Cross-Linked Diels−Alder Polymer Network. *Macromolecules* **2008**, *41*, 9112−9117.

(10) Chen, X.; Dam, M. A.; Ono, K.; Mal, A.; Shen, H.; Nutt, S. R.; Sheran, K.; Wudl, F. A Thermally Re-mendable Cross-Linked Polymeric Material. *Science* **2002**, *295*, 1698−1702.

(11) Reutenauer, P.; Buhler, E.; Boul, P. J.; Candau, S. J.; Lehn, J. M. Room Temperature Dynamic Polymers Based on Diels−Alder Chemistry. *Chem.—Eur. J.* **2009**, *15*, 1893−1900.

(12) Canary, S. A.; Stevens, M. P. Thermally Reversible Crosslinking of Polystyrene Via the Furan−Maleimide Diels−Alder Reaction. *J. Polym. Sci., Part A: Polym. Chem.* **1992**, *30*, 1755−1760.

(13) Liu, Y. L.; Chen, Y. W. Thermally Reversible Cross-Linked Polyamides with High Toughness and Self-Repairing Ability from Maleimide- and Furan-Functionalized Aromatic Polyamides. *Macromol. Chem. Phys.* **2007**, *208*, 224−232.

(14) Tian, Q.; Yuan, Y. C.; Rong, M. Z.; Zhang, M. Q. A Thermally Remendable Epoxy Resin. *J. Mater. Chem.* **2009**, *19*, 1289−1296.

(15) Liu, Y. L.; Chuo, T. W. Self-healing Polymers Based on Thermally Reversible Diels-Alder Chemistry. *Polym. Chem.* **2013**, *4*, 2194−2205.

(16) Gandini, A. The Furan/Maleimide Diels−Alder Reaction: A Versatile Click−Unclick Tool in Macromolecular Synthesis. *Prog. Polym. Sci.* **2013**, *38*, 1−29.

(17) Gandini, A.; Coelho, D.; Silvestre, A. J. D. Reversible Click Chemistry at the service of macromolecular materials. Part 1: Kinetics of the Diels−Alder Reaction Applied to Furan−Maleimide Model Compounds and Linear Polymerizations. *Eur. Polym. J.* **2008**, *44*, 4029−4036.

(18) Gandini, A.; Silvestre, A. J. D.; Coelho, D. Reversible Click Chemistry at the Service of Macromolecular Materials. *Polym. Chem.* **2011**, *2*, 1713−1719.

(19) Gandini, A.; Silvestre, A. J. D.; Coelho, D. Reversible Click Chemistry at the Service of Macromolecular Materials. 2. Thermoreversible Polymers Based on the Diels-Alder Reaction of an A-B Furan/Maleimide Monomer. *J. Polym. Sci., Part A: Polym. Chem.* **2010**, *48*, 2053−2056.

(20) Zhang, Y.; Broekhuis, A. A.; Picchioni, F. Thermally Self-Healing Polymeric Materials: The Next Step to Recycling Thermoset Polymers? *Macromolecules* **2009**, *42*, 1906−1912.

(21) Yu, S.; Zhang, R.; Wu, Q.; Chen, T.; Sun, P. Bio-Inspired High-Performance and Recyclable Cross-Linked Polymers. *Adv. Mater.* **2013**, *25*, 4912−4917.

(22) Johnson, J. C.; Wanasekara, N. D.; Korley, L. T. J. Utilizing Peptidic Ordering in the Design of Hierarchical Polyurethane/Ureas. *Biomacromolecules* **2012**, *13*, 1279−1286.

(23) Mark, J. E.; Eisenberg, A.; Graessley, W. W.; Mandelkern, L.; Koenig, J. *Physical properties of polymers*; Cambridge University Press: UK, 1984.

(24) Chidambareswarapattar, C.; McCarver, P. M.; Luo, H.; Lu, H.; Sotiriou-Leventis, C.; Leventis, N. Fractal Multiscale Nanoporous Polyurethanes: Flexible to Extremely Rigid Aerogels from Multifunctional Small Molecules. *Chem. Mater.* **2013**, *25*, 3205−3224.

(25) Pei, A.; Malho, J.-M.; Ruokolainen, J.; Zhou, Q.; Berglund, L. A. Strong Nanocomposite Reinforcement Effects in Polyurethane Elastomer with Low Volume Fraction of Cellulose Nanocrystals. *Macromolecules* **2011**, *44*, 4422−4427.

(26) Booth, C.; Price, C. *Comprehensive Polymer Science: The Synthesis, Characterization, Reactions & Applications of Polymers*; Pergamon Press: New York, 1989; Vol. 2.

(27) Špírková, M.; Poręba, R.; Pavličević, J.; Kobera, L.; Baldrian, J.; Pekárek, M. Aliphatic Polycarbonate-based Polyurethane Elastomers And Nanocomposites. I. The Influence of Hard-segment Content And Macrodiol-constitution on Bottom-up Self-assembly. *J. Appl. Polym. Sci.* **2012**, *126*, 1016−1030.

(28) Kim, H.-D.; Lee, T. J.; Huh, J. H.; Lee, D. J. Preparation And Properties of Segmented Thermoplastic Polyurethane Elastomers with Two Different Soft Segments. *J. Appl. Polym. Sci.* **1999**, *73*, 345−352.

(29) Castagna, A. M.; Fragiadakis, D.; Lee, H.; Choi, T.; Runt, J. The Role of Hard Segment Content on the Molecular Dynamics of Poly(tetramethylene oxide)-Based Polyurethane Copolymers. *Macromolecules* **2011**, *44*, 7831−7836.

(30) Fragiadakis, D.; Runt, J. Molecular Dynamics of Segmented Polyurethane Copolymers: Influence of Soft Segment Composition. *Macromolecules* **2013**, *46*, 4184−4190.

(31) Yang, Y.; Urban, M. W. Self-healing Polymeric Materials. *Chem. Soc. Rev.* **2013**, *42*, 7446−7467.

(32) Gaina, C.; Ursache, O.; Gaina, V. Re-Mendable Polyurethanes. *Polym.-Plast. Technol. Eng.* **2011**, *50*, 712−718.

(33) Kim, S. Y.; Meyer, H. W.; Saalwächter, K.; Zukoski, C. F. Polymer Dynamics in PEG-Silica Nanocomposites: Effects of Polymer Molecular Weight, Temperature and Solvent Dilution. *Macromolecules* **2012**, *45*, 4225−4237.

(34) Mauri, M.; Thomann, Y.; Schneider, H.; Saalwächter, K. Spin-Diffusion NMR at Low Field for the Study of Multiphase Solids. *Solid State Nucl. Magn. Reson.* **2008**, *34*, 125−141.

(35) Papon, A. l.; Saalwächter, K.; Schäler, K.; Guy, L.; Lequeux, F. O.; Montes, H. Low-Field NMR Investigations of Nanocomposites: Polymer Dynamics and Network Effects. *Macromolecules* **2011**, *44*, 913−922.

(36) Bärenwald, R.; Champouret, Y.; Saalwächter, K.; Schäler, K. Determination of Chain Flip Rates in Poly(ethylene) Crystallites by Solid-State Low-Field 1H NMR for Two Different Sample Morphologies. *J. Phys. Chem. B* **2012**, *116*, 13089−13097.

(37) Demco, D. E.; Johansson, A.; Tegenfeldt, J. Proton Spin Diffusion for Spatial Heterogeneity and Morphology Investigations of Polymers. *Solid State Nucl. Magn. Reson.* **1995**, *4*, 13−38.
(38) Schmidt-Rohr, K.; Clauss, J.; Blümich, B.; Spiess, H. W. Miscibility of Polymer Blends Investigated by 1H Spin Diffusion and 13C NMR Detection. *Magn. Reson. Chem.* **1990**, *28*, S3−S9.
(39) Clauss, J.; Schmidt-Rohr, K.; Spiess, H. W. Determination of Domain Sizes in Heterogeneous Polymers by Solid-State NMR. *Acta Polym.* **1993**, *44*, 1−17.
(40) Saalwächter, K. Proton Multiple-Quantum NMR for the Study of Chain Dynamics and Structural Constraints in Polymeric Soft Materials. *Prog. Nucl. Magn. Reson. Spectrosc.* **2007**, *51*, 1−35.
(41) Baum, J.; Pines, A. NMR Studies of Clustering in Solids. *J. Am. Chem. Soc.* **1986**, *108*, 7447−3454.
(42) Fechete, R.; Demco, D. E.; Blümich, B. Segmental Anisotropy in Strained Elastomers by 1H NMR of Multipolar Spin States. *Macromolecules* **2002**, *35*, 6083−6085.
(43) Saalwächter, K. Microstructure And Molecular Dynamics of Elastomers as Studied by Advanced Low-Resolution Nuclear Magnetic Resonance Methods. *Rubber Chem. Technol.* **2012**, *85*, 350−386.
(44) Chávez, F. V.; Saalwächter, K. NMR Observation of Entangled Polymer Dynamics: Tube Model Predictions and Constraint Release. *Phys. Rev. Lett.* **2010**, *104*, 198305.
(45) Chásse, W.; Valentin, J. L.; Genesky, G. D.; Cohen, C.; Saalwachter, K. Precise Dipolar Coupling Constant Distribution Analysis in Proton Multiple-Quantum NMR of Elastomers. *J. Chem. Phys.* **2011**, *134*, 044907.
(46) Lange, F.; Schwenke, K.; Kurakazu, M.; Akagi, Y.; Chung, U.-i.; Lang, M.; Sommer, J. U.; Sakai, T.; Saalwächter, K. Connectivity and Structural Defects in Model Hydrogels: A Combined Proton NMR and Monte Carlo Simulation Study. *Macromolecules* **2011**, *44*, 9666−9674.
(47) Zhang, R.; Yan, T.; Lechner, B.-D.; Schröter, K.; Liang, Y.; Li, B.; Furtado, F.; Sun, P.; Saalwächter, K. Heterogeneity, Segmental and Hydrogen Bond Dynamics, and Aging of Supramolecular Self-Healing Rubber. *Macromolecules* **2013**, *46*, 1841−1850.
(48) Schmidt-Rohr, K.; Clauss, J.; Spiess, H. W. Correlation of Structure, Mobility, and Morphological Information in Heterogeneous Polymer Materials by Two-Dimensional Wideline-Separation NMR Spectroscopy. *Macromolecules* **1992**, *25*, 3273−3277.
(49) Schmidt-Rohr, K.; Spiess, H. W. *Multidimensional solid-state NMR and polymers*; Academic Press: London, 1994.
(50) Sun, P. C.; Dang, Q. Q.; Li, B. H.; Chen, T. H.; Wang, Y. N.; Lin, H.; Jin, Q. H.; Ding, D. T.; Shi, A. C. Mobility, Miscibility, And Microdomain Structure in Nanostructured Thermoset Blends of Epoxy Resin and Amphiphilic Poly(ethylene oxide)-block-poly(propylene oxide)-block-poly(ethylene oxide) triblock Copolymers Characterized by Solid-State NMR. *Macromolecules* **2005**, *38*, 5654−5667.
(51) Li, X. J.; Fu, W. G.; Wang, Y. N.; Chen, T. H.; Liu, X. H.; Lin, H.; Sun, P. C.; Jin, Q. H.; Ding, D. T. Solid-state NMR Characterization of Unsaturated Polyester Thermoset Blends Containing PEO-PPO-PEO Block Copolymers. *Polymer* **2008**, *49*, 2886−2897.
(52) Dixon, W. T. Spinning-Sideband-Free And Spinning-Sideband-Only NMR Spectra in Spinning Samples. *J. Chem. Phys.* **1982**, *77*, 1800−1809.
(53) Fung, B. M.; Khitrin, A. K.; Ermolaev, K. An Improved Broadband Decoupling Sequence for Liquid Crystals and Solids. *J. Magn. Reson.* **2000**, *142*, 97−101.
(54) Maus, A.; Hertlein, C.; Saalwächter, K. A Robust Proton NMR Method to Investigate Hard/Soft Ratios, Crystallinity, and Component Mobility in Polymers. *Macromol. Chem. Phys.* **2006**, *207*, 1150−1158.
(55) Sommer, J. U.; Saalwächter, K. Segmental Order in End-linked Polymer networks: A Monte Carlo Study. *Eur. Phys. J. E* **2005**, *18*, 167−182.
(56) Chassé, W.; Saalwächter, K.; Sommer, J.-U. Thermodynamics of Swollen Networks As Reflected in Segmental Orientation Correlations. *Macromolecules* **2012**, *45*, 5513−5523.
(57) Saalwachter, K.; Chasse, W.; Sommer, J.-U. Structure and Swelling of Polymer Networks: insights from NMR. *Soft Matter* **2013**, *9*, 6587−6593.
(58) Kennemur, J. G.; Hillmyer, M. A.; Bates, F. S. Rheological Evidence of Composition Fluctuations in an Unentangled Diblock Copolymer Melt near the Order−Disorder Transition. *ACS Macro Lett.* **2013**, *2*, 496−500.
(59) Pongkitwitoon, S.; Hernández, R.; Weksler, J.; Padsalgikar, A.; Choi, T.; Runt, J. Temperature Dependent Microphase Mixing of Model Polyurethanes with Different Intersegment Compatibilities. *Polymer* **2009**, *50*, 6305−6311.
(60) Chen, X.; Wudl, F.; Mal, A. K.; Shen, H.; Nutt, S. R. New Thermally Remendable Highly Cross-Linked Polymeric Materials. *Macromolecules* **2003**, *36*, 1802−1807.
(61) Bloembergen, N.; Purcell, E. M.; Pound, R. V. Relaxation Effects in Nuclear Magnetic Resonance Absorption. *Phys. Rev.* **1948**, *73*, 679−712.
(62) Slichter, C. P. *Principles of Magnetic Resonance*; Springer-Verlag: New York, 1990.
(63) Yamaguchi, M.; Ono, S.; Terano, M. Self-repairing Property of Polymer Network with Dangling Chains. *Mater. Lett.* **2007**, *61*, 1396−1399.
(64) Yu, W.; Du, M.; Zhang, D.; Lin, Y.; Zheng, Q. Influence of Dangling Chains on Molecular Dynamics of Polyurethanes. *Macromolecules* **2013**, *46*, 7341−7351.